PNC TN8410 95−313

NMRによるCMPO/TBP系における ランタニド錯体の構造解析

Study of lanthanide(III) nitrate complexes in CMPO/TBP systems by Nuclear Magnetic Resonance

１９９５年１０月

動力炉・核燃料開発事業団
東　海　事　業　所

PNC TN8410 95－313
１９９５年１０月

NMRによるCMPO/TBP系におけるランタニド錯体の構造解析

Study of lanthanide(III) nitrate complexes in CMPO/TBP systems by Nuclear Magnetic Resonance

佐野雄一*、狩野純一**、青瀬晋一*
岡本文敏*、田中康正*

要　旨

TRUEX (transuranium extraction) プロセスにおいて使用される抽出剤 CMPO (octyl(phenyl)-N,N-diisobutylcarbamoylmethylphosphine oxide)及び相改質剤 TBP (tributylphosphate)と軽ランタニド元素（La, Ce, Pr, Nd, Sm, Eu）との反応について、NMR（核磁気共鳴吸収）測定を用いて検討を行った。

NMR 測定の結果より、ランタニド/TBP 系においては２分子の TBP が、ランタニド/CMPO 系においては３分子の CMPO が、それぞれランタニドイオンに単座配位及び２座配位することが示された。また、ランタニド/CMPO/TBP 系においては、CMPO のみが直接ランタニドイオンに２座配位し、TBP は第一配位圏には存在しないことが確認された。

ランタニド/TBP 系及びランタニド/CMPO 系における配位子交換反応については、CBS (complete bandshape)法から求められた活性化パラメータの値から、会合機構あるいは第 1 配位圏外での溶媒などとの相互作用を伴う解離機構により配位子交換反応が進むものと推測された。一方、ランタニド/CMPO/TBP 系における CMPO の交換反応は、第１配位圏外での TBP による影響を伴った反応で進行することが示唆された。

---

* 再処理技術開発部　アクチニドプロセス・分析開発室
** 検査開発㈱

PNC TN8410 95－313

October , 1995

Study of lanthanide(III) nitrate complexes in CMPO/TBP systems by Nuclear Magnetic Resonance

Yuichi Sano*, Jun-ichi Karino**, Shin-ichi Aose*,
Fumitoshi Okamoto* and Yasumasa Tanaka*

ABSTRACT

The coordination properties of the lanthanide (La, Ce, Pr, Nd, Sm and Eu) complexes in lanthanide/TBP (tributylphosphate), lanthanide/CMPO (octyl(phenyl)-N,N-diisobutylcarbamoylmethylphosphine oxide) and lanthanide/CMPO/TBP systems were investigated by the NMR (nuclear magnetic resonance) measurements.

The numbers of the coordinated CMPO and TBP to the lanthanide ion were estimated about three and two in the lanthanide/CMPO and lanthanide/TBP systems, respectively. It is considered that TBP and CMPO coordinate to the lanthanide(III) ion in the monodentate and the bidentate manners, respectively. In the lanthanide/CMPO/TBP system, ^{31}P-NMR spectra suggested that CMPO coordinates to lanthanide(III) ion directly in the bidentate mode, but TBP doesn't exist within the first coordination sphere and coordinates to the lanthanide(III) ion from beyond the first coordination sphere.

The activation parameters for the ligand exchange reactions calculated by the CBS (complete bandshape) method suggest that the ligand exchange reactions in the lanthanide (Pr and Eu)/TBP and lanthanide (La, Pr and Sm)/CMPO systems proceed through either the associative (A) mechanism or the dissociative (D) mechanism with an ordering into the second coordination sphere. In the lanthanide (Pr and Sm)/CMPO/TBP systems, it was shown that the CMPO exchange reactions proceed through the mechanism with an ordering into the second coordination sphere, which is caused by TBP in the systems.

---

* Power Reactor and Nuclear Fuel Development Corporation, Tokai, Ibaraki, 319-11, Japan

** Inspection Development Company Ltd., Tokai, Ibaraki, 319-11, Japan

CONTENTS

LIST OF TABLES

LIST OF FIGURES

1. INTRODUCTION

In an existing nuclear fuel cycle process, the PUREX (plutonium uranium reduction extraction) process is mainly used for a fuel reprocessing, which recovers uranium and plutonium from an acidic dissolver solution of spent nuclear fuel by a liquid-liquid extraction using TBP (tributylphosphate). In the PUREX process, uranium and plutonium can be obtained in high purity, HLLW (high level liquid wastes), however, still contains burnable MA (minor actinides) and long-lived FPs (fission products).

Recently, the recycle of minor actinide elements, so-called "Actinide Recycle" concept, is arisen, which aims at the cost-effective management and disposal of HLLW and the nuclear nonproliferation by mixing them into plutonium, and recovery processes for the removal of actinides from spent nuclear fuel have been studied. Based on the extraction process, some partitioning processes of actinide elements from HLLW are developed up to now[1)-4)]. Among these processes, TRUEX (transuranium extraction) process developed in ANL of USA uses CMPO (octyl(phenyl)-N,N-diisobutylcarbamoylmethylphosphine oxide) as an extractant diluted into n-dodecane containing TBP as a phase modifier, so it has a good compatibility with the composition of the organic phase in the PUREX process (30% TBP in n-dodecane). In the TRUEX process, trivalent lanthanides contained as FPs are coextracted with MA from HLLW. Therefore, in order to evaluate this process correctly, it is important to evaluate an extraction behavior of not only actinides but also lanthanides.

The details of the coordination structure of extracted complexes and the kinetics of extractants lead to a deeper understanding of the extraction mechanism, so these have been studied in lanthanide/TBP and lanthanide/CMPO systems[5)-7)]. But there are few studies concerned with the coordination structures and the kinetics of the complexes in lanthanide/CMPO/TBP system. NMR (nuclear magnetic resonance) spectroscopy is one of the useful methods for the elucidation of the structure and dynamics of the complexes in such mixed liquid systems. In this study, coordination properties of the complexes in the lanthanide/TBP, lanthanide/CMPO and lanthanide/CMPO/TBP systems are investigated by NMR measurements.

2. EXPERIMENTAL

2.1 Materials

We selected light lanthanide elements as samples, which have large fission yields, and hydrated lanthanide(III) nitrates (La, Ce, Pr, Nd, Sm and Eu) were purchased

from Soekawa Chemicals LTD. These materials were reagent grade. TBP and CMPO purchased from Wako Pure Chemical Industries LTD and Atochem North America, respectively, were used without further purification.

2.2 NMR Measurements

NMR measurements for ^{13}C and ^{31}P were performed on a JEOL LA-400 NMR spectrometer with a duterium lock ($CDCl_3$) at 100.4 MHz and 161.7 MHz for ^{13}C and ^{31}P, respectively . The ^{13}C-NMR chemical shifts were measured with respect to TMS as an internal reference and the ^{31}P-NMR chemical shifts were measured with respect to 85% H_3PO_4 solution as an external reference. The assignments of ^{13}C-NMR signals for TBP, CMPO and the complexes were made by C-H COSY 2D-NMR and DEPT spectra. The sample solutions were prepared by mixing an appropriate amount of hydrated lanthanide(III) nitrate, TBP and CMPO into a proper quantity of $CDCl_3$. The concentrations of these materials were based on those in the HLLW and TRUEX process, and prepared by considering the condition for the NMR measurements. All NMR measurements were performed in $CDCl_3$ after bubbling argon gas through the samples for 5 minutes.

3. RESULTS AND DISCUSSION

3.1 Coordination structures of lanthanide complexes in lanthanide/TBP, lanthanide/CMPO and lanthanide/CMPO/TBP systems

Figure 3.1 shows ^{31}P-NMR spectra of free TBP and in lanthanide (Pr and Nd)/TBP systems. In ^{31}P-NMR spectra on lanthanide/TBP systems, both the peaks of free TBP and lanthanide-TBP complexes are obtained, because the TBP exchange between the free and the coordinated states is slow with respect to the ^{31}P-NMR time scale under these conditions. The difference of the chemical shifts between them suggests that the magnetic environment of phosphorus atom has been changed by the bond of lanthanide (III) ion with the phosphoryl oxygen in TBP. Figure 3.2 shows ^{31}P-NMR spectra of free CMPO and in lanthanide (La and Sm)/CMPO systems. Similarly to the measurement results in lanthanides/TBP systems, the difference of the chemical shifts between free CMPO and lanthanide/CMPO complexes is observed, which suggests the change of the magnetic environment of phosphorus atom on the complexation.

Each ^{31}P-NMR spectrum shown in Fig. 3.3 and Fig. 3.4 were measured by changing the concentration ratio of the lanthanide(III) ion (Eu or Ce) to TBP or CMPO. In those spectra, the peaks at up-field and down-field are assigned to free TBP or CMPO

and coordinated TBP or CMPO, respectively. The ratios of the integrated areas for the free TBP or CMPO and coordinated TBP or CMPO represent their abundance ratios, so the number of the coordinated TBP or CMPO can be calculated by the mole ratio for the added TBP or CMPO to the lanthanide ion, and by the ratio of the integrated areas for these peaks. As shown in Fig. 3.3 and Fig 3.4, in these conditions, where the concentration of the free TBP or CMPO is much higher than that of lanthanide ion, the numbers of the coordinated TBP and CMPO are calculated as about two and three, respectively. The same coordination number was obtained in other lanthanide-TBP or lanthanide-CMPO complexes.

Figure 3.5 shows ^{13}C-NMR spectra of free CMPO and in lanthanide (La and Nd)/CMPO systems. These ^{13}C-NMR spectra were assigned using a C-H COSY and DEPT spectra (Fig. 3.6(a) and Fig. 3.6(b)). The peaks for free CMPO, La/CMPO and Nd-CMPO complexes observed at 165, 168 and 180 ppm, respectively, are assigned to the carbonyl carbon. These signals shift to down-field from that of free CMPO, which suggests the contribution of carbonyl group to the bond between lanthanide(III) ions and CMPO. Figure 3.7 shows a temperature dependence of ^{31}P-NMR spectra in Nd/CMPO system. As seen from this figure, the signal assigned to Nd-CMPO complex is a single peak at a high temperature, but this peak splits into several peaks following the decrease of temperature. This phenomenon suggests the existence of several isomers based on the bidentate coordination of unsymmetrical CMPO to lanthanide(III) ion, which exchange each other more rapidly than the ^{31}P-NMR time scale at the high temperature[8]. On the other hand, only a single ^{31}P-NMR peak for Nd-TBP complex is obtained at any temperature as shown in Fig 3.8 because of a monodentate coordination of TBP. From the above-mentioned, it is considered that TBP coordinates to a lanthanide(III) ion in the monodentate manner in the lanthanide/TBP system and CMPO coordinates to a lanthanide(III) ion in the bidentate manner in the lanthanide/CMPO system.

Figure 3.9 shows ^{31}P-NMR spectra in Nd/CMPO/TBP system at -30°C. In this figure, the same peaks for the several isomers of the Nd-CMPO complexes as those were obtained in the Nd/CMPO system, are observed, but the signal of the Nd-TBP complex can not be observed. For the Eu/CMPO/TBP system, a similar result, which suggests the existence of the only Eu-CMPO complex, is obtained as shown in Fig. 3.10. Figure 3.11 shows the ^{31}P-NMR signals of free CMPO and the Sm-CMPO complex in the Sm/CMPO/TBP system. From the mole ratio for the added CMPO and samarium(III) ion and the ratio of the integrated areas for these peaks, the coordination number of CMPO to samarium(III) ion is calculated as about three and it is confirmed that the number of coordinated CMPO don't change between the Sm/CMPO and

Sm/CMPO/TBP systems. These experimental results suggest that only CMPO coordinates to lanthanide(III) ion directly in the bidentate mode and TBP doesn't exist within the first coordination sphere in the lanthanide(III)/CMPO/TBP system. But it is considered that TBP may coordinate to lanthanide(III) ion from beyond the first coordination sphere, because the slightly ^{31}P-NMR chemical shift of TBP is observed in the lanthanide/CMPO/TBP system shown in Fig. 3.12.

3.2 Ligand exchange reactions in the lanthanide/TBP, lanthanide/CMPO and lanthanide/CMPO/TBP systems

Figure 3.13 shows the temperature dependence of ^{31}P-NMR spectra in La/CMPO systems. In this temperature range, the exchange reaction between the isomers of La-CMPO complex is so rapid that the signals of them coalesce into a single peak, but the exchange reaction between free CMPO and the La-CMPO complex can be observed from their ^{31}P-NMR spectra shown in this figure. The ^{31}P-NMR signals assigned to free CMPO and the La-CMPO complex are obtained separately at the low temperature and the exchange reaction between them becomes more rapid at the high temperature, so these peaks are coalescing as the temperature rises. The change of ^{31}P-NMR spectra by such a ligand exchange reaction is also obtained in the other lanthanide/TBP and lanthanide/CMPO systems (Figure 3.14 shows the temperature dependence of ^{31}P-NMR spectra in Pr/CMPO system).

To determine activation parameters of the ligand exchange reactions in these systems, the CBS (complete bandshape) method based on an uncoupled two-site exchange case was used in this study. The bandshape, v, for an uncoupled two-site exchange system is given by equation 3.1[9],

$$v = -C_0 \frac{\left\{P\left[1+\tau\left(\frac{p_B}{T_{2A}}+\frac{p_A}{T_{2B}}\right)\right]+QR\right\}}{P^2+R^2} \qquad (3.1)$$

$$\delta\nu = \nu_A - \nu_B, \quad \Delta\nu = 0.5(\nu_A+\nu_B)-\nu$$

$$P = \tau\left[\frac{1}{T_{2A}\cdot T_{2B}} - 4\pi^2\Delta\nu^2 + \pi^2(\delta\nu)^2\right] + \frac{p_A}{T_{2A}} + \frac{p_B}{T_{2B}}$$

$$Q = \tau\left[2\pi\Delta\nu - \pi\delta\nu(p_A - p_B)\right]$$

$$R = 2\pi\Delta\nu\left[1+\tau\left(\frac{1}{T_{2A}}+\frac{1}{T_{2B}}\right)\right] + \pi\delta\nu\tau\left(\frac{1}{T_{2B}}-\frac{1}{T_{2A}}\right) + \pi\delta\nu(p_A - p_B)$$

$$\tau = \frac{p_A}{k_B} = \frac{p_B}{k_A}$$

where p_A and p_B are the fractional populations of nuclei in sites A and B ($p_A + p_B = 1$), k_A and k_B are the rate constants which give the probability for a jump from site A and B, respectively, ν_A and ν_B are the resonance frequencies of nuclei in site A and B, and T_{2A} and T_{2B} are the transverse relaxation times of nuclei in site A and B, which are calculated approximately by equation, $T_2 = 1/\pi W$, where W is a halfwidth of the signal in each site, respectively. The bandshape, v, is visualized using a personal computer from equation 3.1 by entering ν_A, ν_B, p_A, p_B, the corresponding T_2 values, and a trial k value. The optimum exchange rate constant can be obtained by the fitting of the calculated spectra on the experimental spectra at each temperature. Figure 3.15 shows the experimental ^{31}P-NMR spectra of the La/CMPO system and simulated best fit spectra calculated by equation 3.1 at various temperatures. The derived exchange rate constant, k, are collected in Table 3.1. The relationship between the exchange rate constant, k, and absolute temperature, T, is given by the Eyring equation (3.2).

$$k = \kappa \frac{k_B T}{h} e^{-\Delta G^{\#}/RT} \qquad (3.2a)$$

$$k = \kappa \frac{k_B T}{h} e^{(\Delta H^{\#} - T\Delta S^{\#})/RT} \qquad (3.2b)$$

Here k_B and h denote the Boltzmann constant and Planck constant, respectively, and κ is the transmission coefficient, i.e. the fraction of all reacting molecules reaching the transition state that proceed to deactivated product molecules. In adiabatic reaction, the magnitude of κ is determined by the capacity of the activated complex to transfer the activation energy to other molecules. Normally this proceeds so smoothly with polyatomic molecules that κ can be assumed to be close to, or equal to, unity, and equation 3.3 is obtained.

$$\ln\frac{k}{T} = -\frac{\Delta G^{\#}}{RT} - \ln\frac{h}{k_B} \qquad (3.3a)$$

$$\ln\frac{k}{T} = -\frac{\Delta H^{\#}}{RT} + \frac{\Delta S^{\#}}{R} - \ln\frac{h}{k_B} \qquad (3.3b)$$

The activation parameters, $\Delta G^{\#}$, $\Delta H^{\#}$ and $\Delta S^{\#}$, are determined by a least-squares adaptation of equation 3.3 to a linear plot of $\ln(k/T)$ vs. 1/T. Figure 3.16 shows the plot of $\ln(k/T)$ vs. 1/T in La/CMPO and Pr/TBP systems, and the parameters characterizing ligand exchange in lanthanide (La, Pr and Sm)/CMPO and lanthanide (Pr and Eu)/TBP systems are summarized with the ionic radii of the lanthanide (III) ions in Table 3.2. It is seen that k (300K) decreases and $\Delta H^{\#}$ increases as the ionic radius of the lanthanide ion

decreases. The variation of $\Delta H^{\#}$ is consistent with the electrostatic attraction between the metal ion and CMPO or TBP decreasing as the ionic radius of the lanthanide ion increases. In the lanthanide/CMPO and lanthanide/TBP systems, $\Delta S^{\#}$ are negative within experimental errors, so it is considered that the ligand exchange reactions in these systems proceed through an associative (A) mechanism given in equation 3.4,

$$\left[Ln(NO_3)_3 \cdot nE\right] + {}^*E \rightarrow \left[Ln(NO_3)_3 \cdot nE\right] \cdot {}^*E \qquad (3.4a)$$

$$\left[Ln(NO_3)_3 \cdot nE\right] \cdot {}^*E \rightarrow \left[Ln(NO_3)_3 \cdot (n-1)E \cdot {}^*E\right] + E \qquad (3.4b)$$

or a dissociative (D) mechanism given in equation 3.5 with an ordering into the second coordination sphere[10), (11)].

$$\left[Ln(NO_3)_3 \cdot nE\right] \rightarrow \left[Ln(NO_3)_3 \cdot (n-1)E\right] + E \qquad (3.5a)$$

$$\left[Ln(NO_3)_3 \cdot (n-1)E\right] + {}^*E \rightarrow \left[Ln(NO_3)_3 \cdot (n-1)E \cdot {}^*E\right] \qquad (3.5b)$$

where E denotes CMPO or TBP molecule and an asterisk denotes the exchange species.

Figure 3.17 shows the temperature dependence of ^{31}P-NMR spectra for free and coordinated CMPO in Sm/CMPO and Sm/CMPO/TBP systems. The activation parameters calculated by the CBS method for CMPO exchange reaction in Sm/CMPO/TBP and Pr/CMPO/TBP systems are summarized in Table 3.3. It is recognized that k (300K), $\Delta H^{\#}$ and $\Delta S^{\#}$ decrease as the concentration of TBP in the system increases. The variation of $\Delta S^{\#}$ indicates an increased ordering of the transition state with respect to the ground state as TBP concentrations in the system increases. No signal for TBP coordinated to the lanthanide ion directly was observed under these experimental conditions, so this result seems to be caused by the interaction between the lanthanide ion and TBP in the transition state beyond the first coordination sphere. Namely, it is considered that the exchange reactions of CMPO in Sm/CMPO/TBP and Pr/CMPO /TBP systems proceed through the mechanism with the ordering into the second coordination sphere, which is caused by TBP in these systems. In the range of low TBP concentration (the mole ratio for added TBP to the lanthanide ion (TBP/Ln) < ~5), the contribution of TBP beyond the first coordination sphere is small, but that becomes larger as the TBP concentration increases. Therefore, it is considered that large negative $\Delta S^{\#}$ values were obtained under the condition of a large amount of TBP existence against few changes of the activation parameters from in the lanthanide/CMPO systems in the low TBP concentration systems. Such an interaction between the lanthanide ion and TBP beyond the first coordination sphere are also recognized by the slightly ^{31}P-

NMR chemical shift of TBP in the lanthanide/CMPO/TBP systems mentioned in the preceding paragraph.

4. CONCLUSION

We investigated the coordination properties of the complexes in the lanthanide/TBP, lanthanide/CMPO and lanthanide/CMPO/TBP systems by using the NMR measurements in this study. The results are summarized as follows:

(1) The numbers of the coordinated CMPO and TBP to the lanthanide(III) ion are estimated about three and two in the lanthanide/CMPO and lanthanide/TBP systems, respectively. TBP and CMPO coordinate to the lanthanide(III) ion in the monodentate and the bidentate manners, respectively.

(2) In the lanthanide/CMPO/TBP system, only CMPO coordinates to lanthanide(III) ion directly in the bidentate mode, and TBP doesn't exist within the first coordination sphere.

(3) The activation parameter for the ligand exchange reactions were obtained in the lanthanide(Pr and Eu)/TBP and lanthanide(La, Pr and Sm)/CMPO systems. The obtained $\Delta S^{\#}$ values suggest that the ligand exchange reactions in these systems proceed through either the associative (A) mechanism or the dissociative (D) mechanism with an ordering into the second coordination sphere.

(4) In the lanthanide(Pr and Sm)/CMPO/TBP systems, the CMPO exchange reactions proceed through the mechanism with an ordering into the second coordination sphere, which is caused by TBP in the systems.

We will research the coordination properties of the lanthanide complexes in the TRUEX process (CMPO/TBP/n-dodecane), especially the structure and the formation mechanism of the third phase, by the NMR measurements hereafter.

REFERENCES

(1) W. W. Schulz and E. P. Horwitz, *Sep. Sci. Technol.*, **26**, 1191 (1988).

(2) C. Madic, P. Blanc, N. Condamines, P. Baron, L. Berthon, C. Nicol, C. Pozo, M. Lecomte, M. Philippe, M. Masson, C. Hequet and M. J. Hudson, *Proceedings of "RECOD '94" London*, vol.3, (1994).

(3) Y. Morita and M. Kubota, *J. Nucl. Sci. Technol.*, **22**, 658 (1985).

(4) Y. Zhu, C. Song, J. Xu, D. Yang, B. Lie and J. Chen, *Chinese Journal of Nucl. Sci. Eng.*, **9**, 141 (1989).

(5) S. Z. Ndzuta, E. W. Giesekke and K. G. R. Pachler, *J. Inorg. Nucl. Chem.*, **42**, 1067 (1979).

(6) T. Nakamura and C. Miyake, *Solv. Extr. Ion Exch.*, **12**, 931 (1994).

(7) T. Nakamura and C. Miyake, *Solv. Extr. Ion Exch.*, **12**, 951 (1994).

(8) T. Nakamura and C. Miyake, *Solv. Extr. Ion Exch.*, **12**, 931 (1994).

(9) J. Sandström, *Dynamic NMR Spectroscopy*, Academic Press (1982).

(10) S. F. Lincoln and A. White, *Polyhedron*, **5**, 1351 (1986).

(11) S. F. Lincoln, A. M. Hounslow and A. J. Jones, *Aust. J. Chem.*, **35**, 2393 (1982).

Table 3.1 Exchange rate constants on lanthanide (III) ions

Ln^{3+}	k (s^{-1})										
	-50°C	-45°C	-40°C	-35°C	-30°C	-25°C	-20°C	-15°C	-10°C	-5°C	0°C
						$Ln(NO_3)_3$·3CMPO(*a)					
La^{3+}	26	46	78	138	229	382	618	919	1.5×10^3	2.3×10^3	3.3×10^3
Pr^{3+}(*1)								544	829	1.3×10^3	1.9×10^3
Sm^{3+}						121	199	319	524	758	1.2×10^3
						$Ln(NO_3)_3$·2TBP(*b)					
Pr^{3+}	232	362	502	743	1.1×10^3	1.7×10^3	2.5×10^3	3.8×10^3			
Eu^{3+}				263	378	569	854	1.2×10^3	1.9×10^3	2.7×10^3	

(*a) The exchange rate constants were obtained in the system where the mole ratio for CMPO to the lanthanide ion is about 5.5.

(*b) The exchange rate constants were obtained in the system where the mole ratio for TBP to the lanthanide ion is about 4.8.

(*1) For the Pr/CMPO system, 2.9×10^2 (s^{-1}) and 4.3×10^2 (s^{-1}) were obtained as the exchange rate constants at 5°C and 10°C, respectively.

Table 3.2 Parameters for ligand exchange reaction on lanthanide (III) ions(*1)

Ln^{3+}	r (nm)	k (300K) (s^{-1})	$\Delta H^{\#}$ (kJ/mol)	$\Delta S^{\#}$ (J/mol·K)
		$Ln(NO_3)_3$·3CMPO(*a)		
La^{3+}	0.117	$(2.5\pm0.03)\times10^4$	47.4±0.3	-3.2±1.1
Pr^{3+}	0.113	$(1.4\pm0.03)\times10^4$	48.1±0.4	-5.1±1.5
Sm^{3+}	0.110	$(8.9\pm0.3)\times10^3$	48.7±0.7	-7.1±2.7
		$Ln(NO_3)_3$·2TBP(*b)		
Pr^{3+}	0.113	$(5.2\pm0.03)\times10^4$	35.8±0.3	-35.4±3.6
Eu^{3+}	0.109	$(2.5\pm0.03)\times10^4$	39.4±0.3	-29.8±3.0

r : ionic radius of lanthanide (III) ions.

(*a) The exchange rate constants were obtained in the system where the mole ratio for CMPO to the lanthanide ion is about 5.5.

(*b) The exchange rate constants were obtained in the system where the mole ratio for TBP to the lanthanide ion is about 4.8.

(*1) Quoted errors represent standard deviations obtained from a linear regression fit of the experimental data to the Eyring equation.

Table 3.3 Parameters for CMPO exchange reaction in Sm/CMPO/TBP and Pr/CMPO/TBP systems(*1)

Sm 0.023M / CMPO 0.13M			
TBP (M)	k (300K) (s^{-1})	$\Delta H^{\#}$ (kJ/mol)	$\Delta S^{\#}$ (J/mol·K)
0.12	$(8.8\pm0.3)\times10^{3}$	49.7±2.5	-4.1±10.3
0.24	$(4.0\pm0.3)\times10^{3}$	39.9±0.8	-43.3±3.1
0.47	$(2.3\pm0.3)\times10^{3}$	36.6±1.6	-58.7±6.0

Pr 0.044M / CMPO 0.24M			
TBP (M)	k (300K) (s^{-1})	$\Delta H^{\#}$ (kJ/mol)	$\Delta S^{\#}$ (J/mol·K)
0.24	$(1.6\pm0.03)\times10^{4}$	48.9±0.7	-1.8±2.8
0.48	$(1.5\pm0.03)\times10^{4}$	48.1±0.7	-4.7±2.7
0.95	$(1.2\pm0.03)\times10^{4}$	42.0±0.6	-27.5±2.3

(*1) Quoted errors represent standard deviations obtained from a linear regression fit of the experimental data to the Eyring equation.

(a) TBP

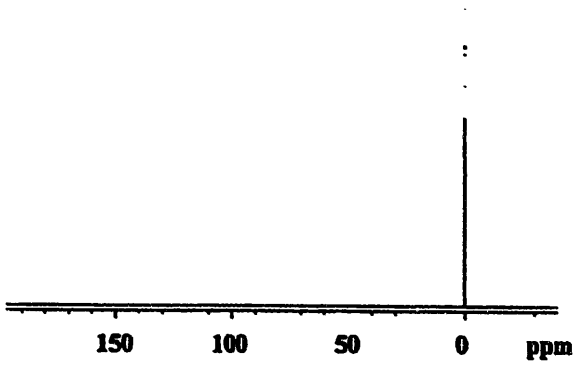

(b) Pr/TBP system

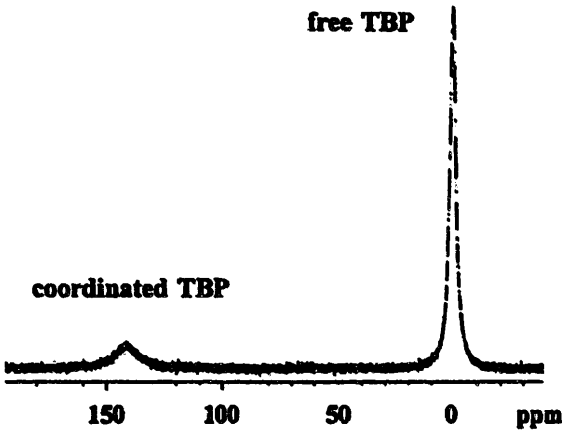

(c) Nd/TBP system

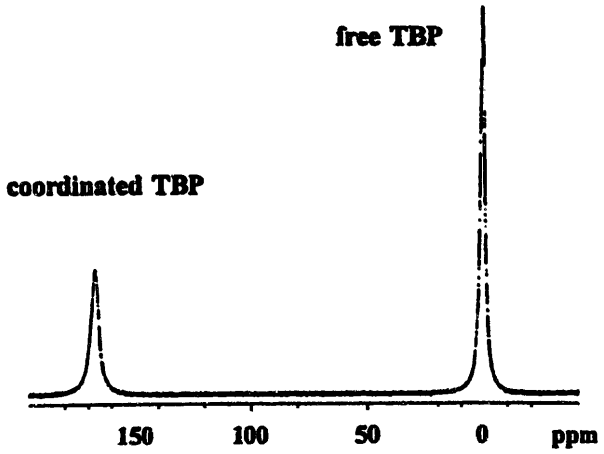

Fig. 3.1 (a) ^{31}P-NMR spectra of TBP at -40 °C.
(b) ^{31}P-NMR spectra in Pr/TBP system at -50 °C.
Concentrations of Pr and TBP are 0.088M and 0.94M, respectively.
(c) ^{31}P-NMR spectra in Nd/TBP system at -40 °C.
Concentrations of Nd and TBP are 0.087M and 0.47M, respectively.

(a) CMPO

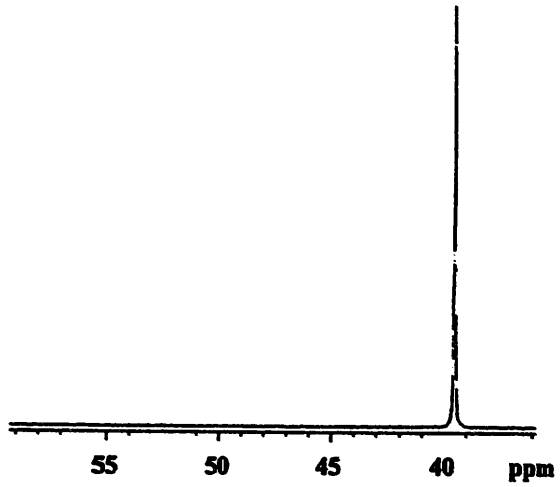

(b) La/CMPO system

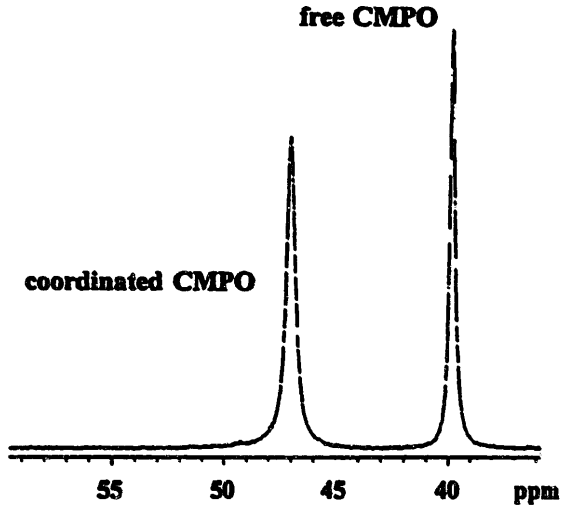

(c) Sm/CMPO system

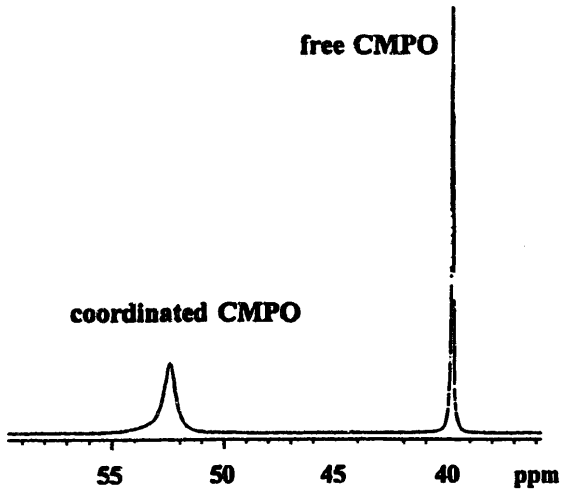

Fig. 3.2 (a) ^{31}P-NMR spectra of CMPO at -40 °C.
(b) ^{31}P-NMR spectra in La/CMPO system at -40 °C.
Concentrations of La and CMPO are 0.086M and 0.47M, respectively.
(c) ^{31}P-NMR spectra in Sm/CMPO system at -40 °C.
Concentrations of Sm and CMPO are 0.086M and 0.47M, respectively.

(a) Eu 0.086M TBP 0.47M

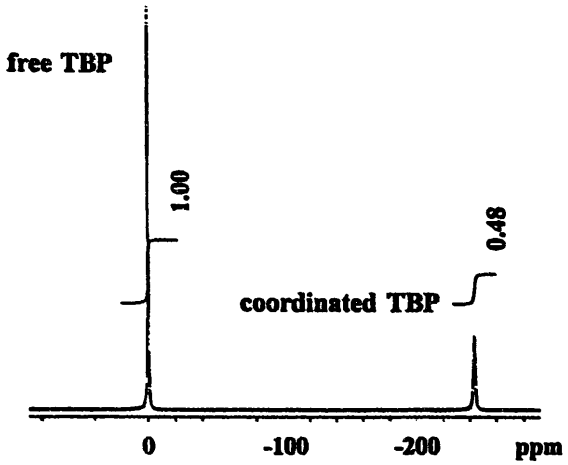

$Eu(NO_3)_3 \cdot nTBP$

$$n = \frac{0.47}{0.086} \cdot \frac{0.48}{1.48} = \underline{1.77}$$

(b) Eu 0.086M TBP 0.70M

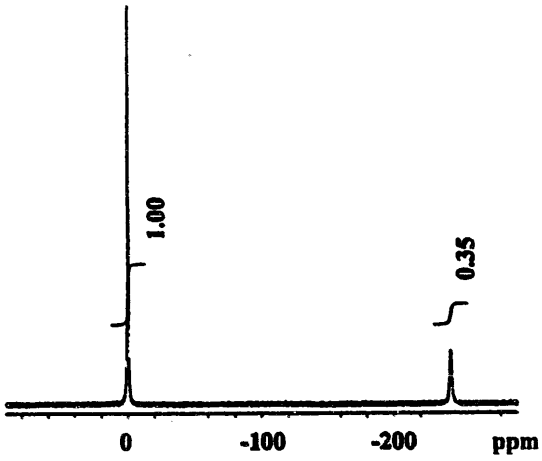

$$n = \frac{0.70}{0.086} \cdot \frac{0.35}{1.35} = \underline{2.11}$$

(c) Eu 0.086M TBP 0.93M

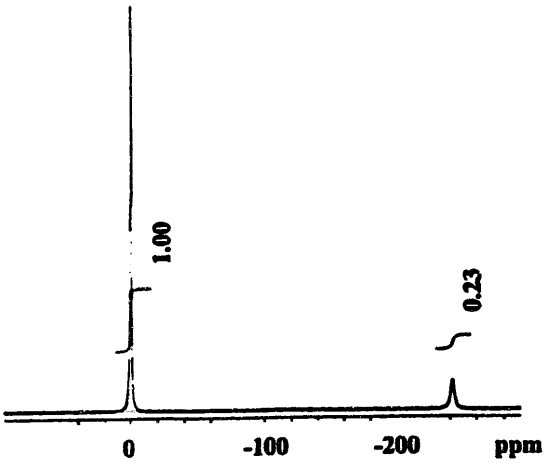

$$n = \frac{0.93}{0.086} \cdot \frac{0.23}{1.23} = \underline{2.02}$$

Fig. 3.3 ^{31}P-NMR spectra in Eu/TBP system at -40 °C.

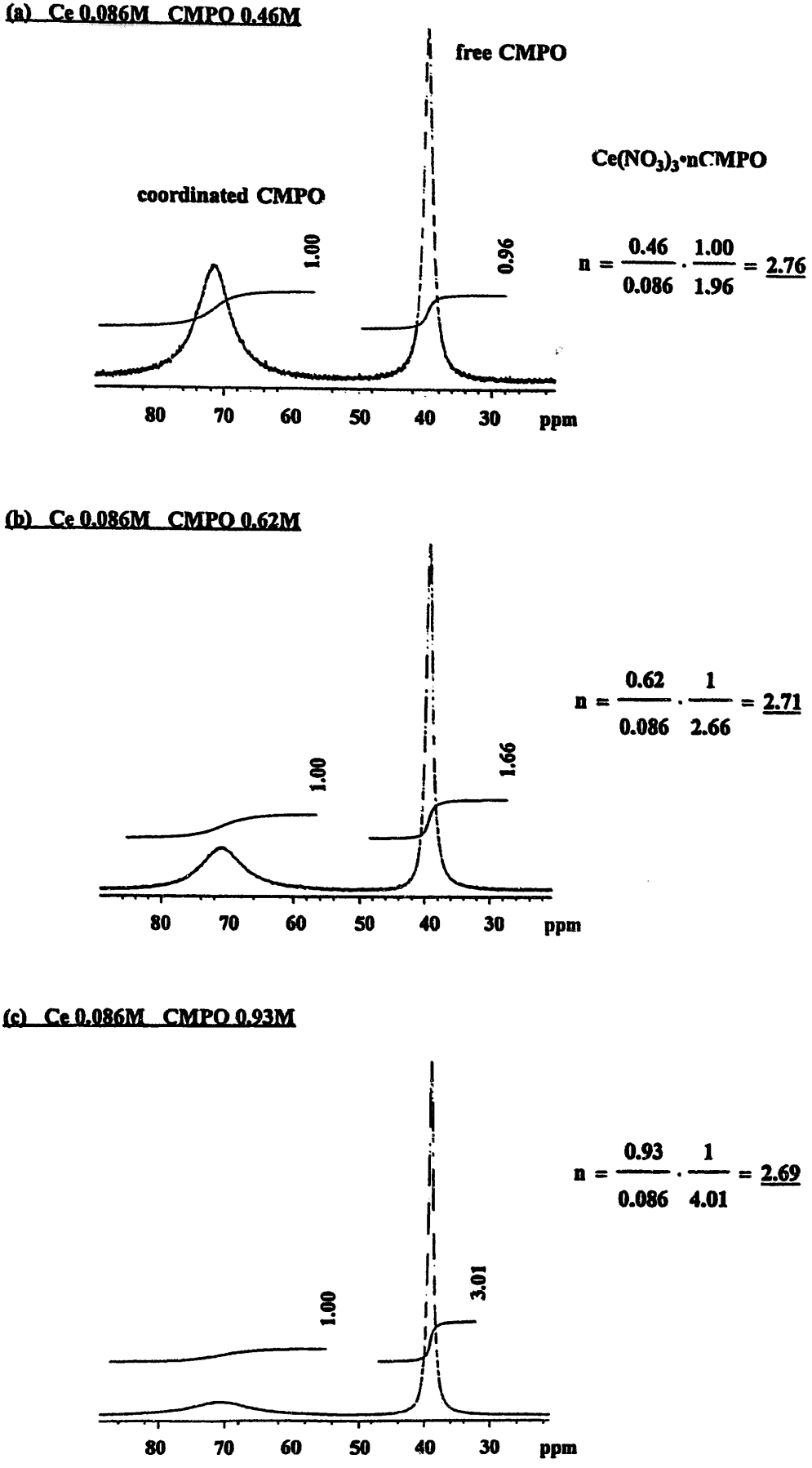

Fig. 3.4 ^{31}P-NMR spectra in Ce/CMPO system at -20 °C.

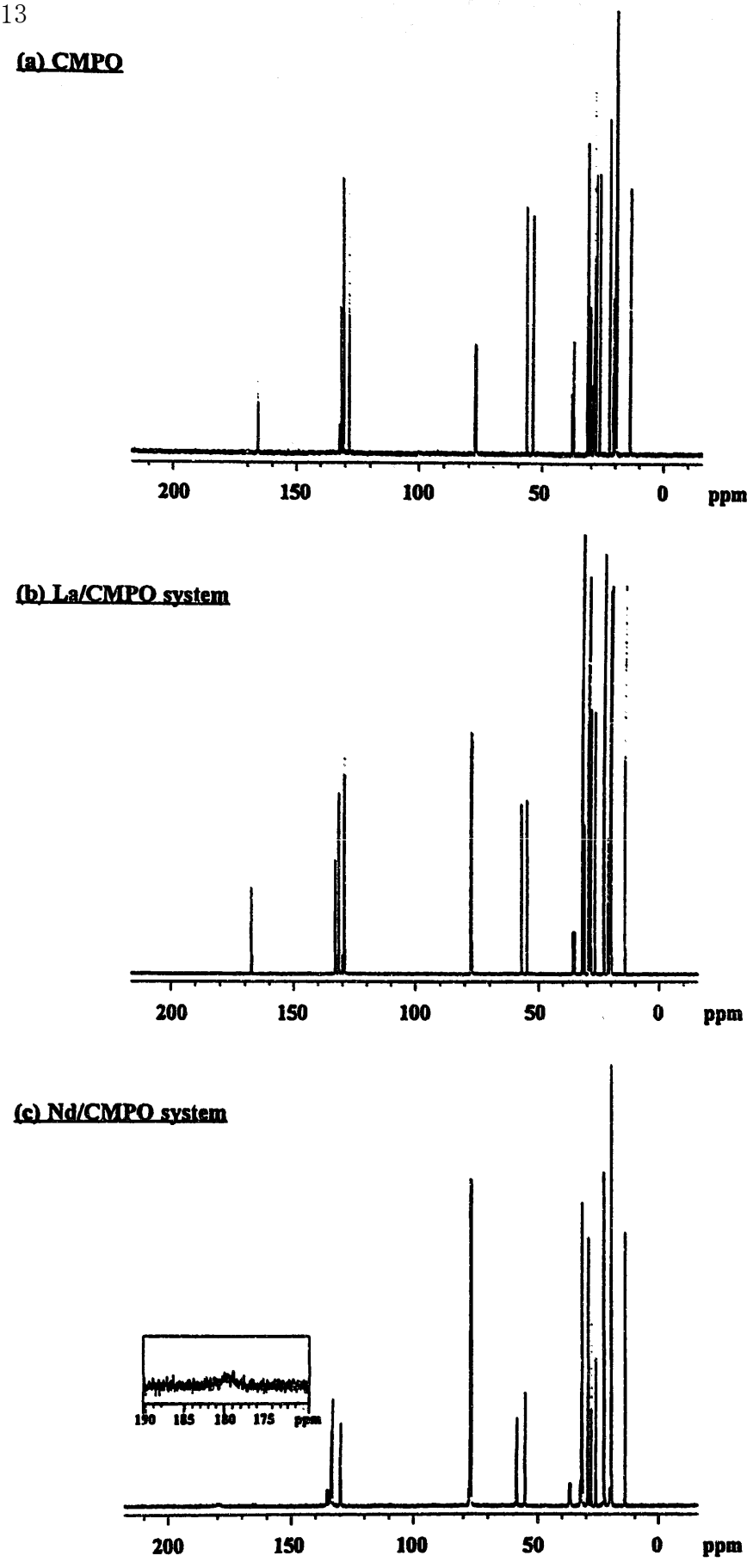

Fig. 3.5 (a) ^{13}C-NMR spectra of CMPO at room temperature.
(b) ^{13}C-NMR spectra in La/CMPO system at room temperature.
Concentrations of La and CMPO are 0.086M and 0.27M, respectively.
(c) ^{13}C-NMR spectra in Nd/CMPO system at room temperature.
Concentrations of Nd and CMPO are 0.087M and 0.27M, respectively

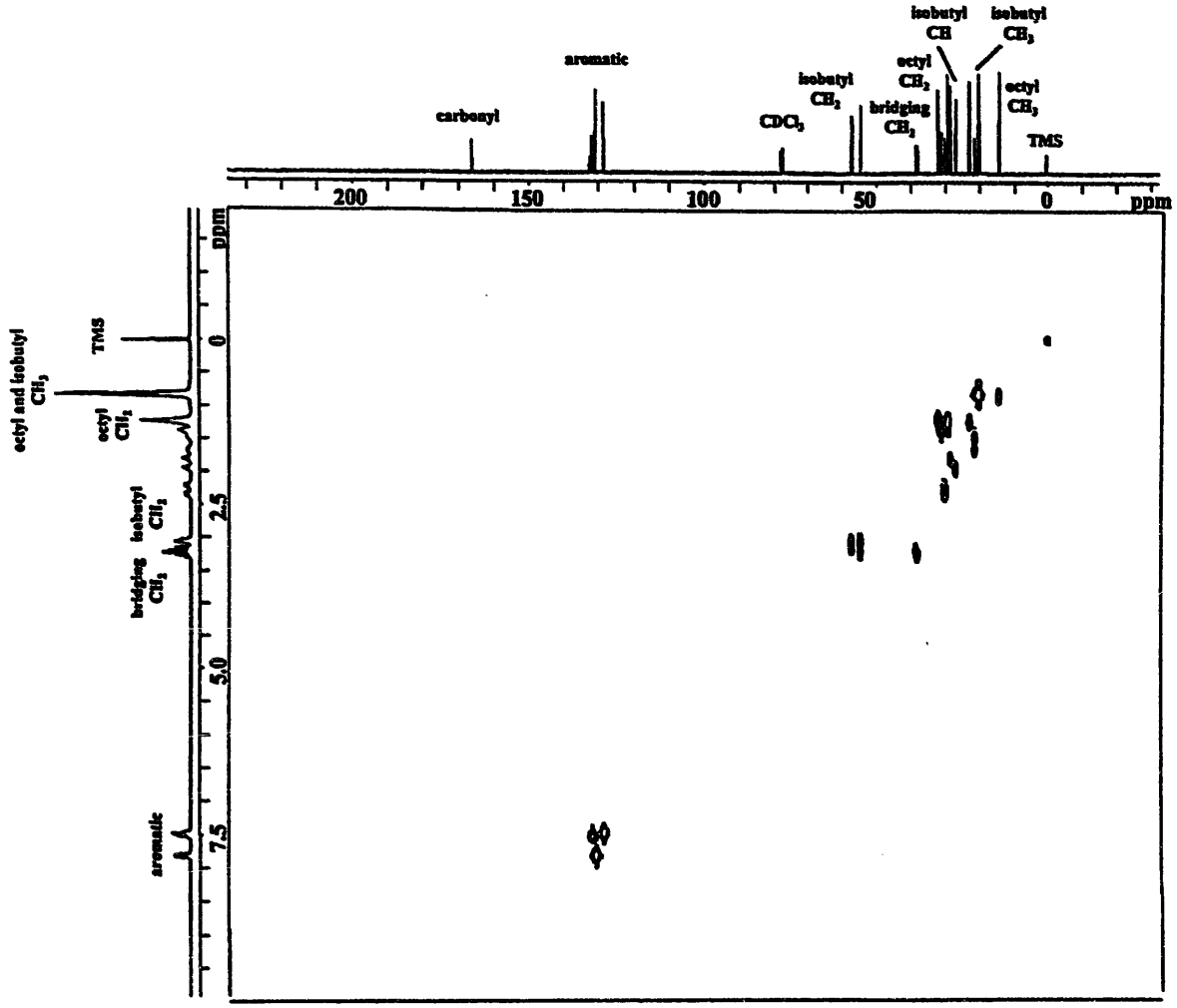

Fig. 3.6 (a)　C-H COSY 2D-NMR spectra of CMPO at room temperature.

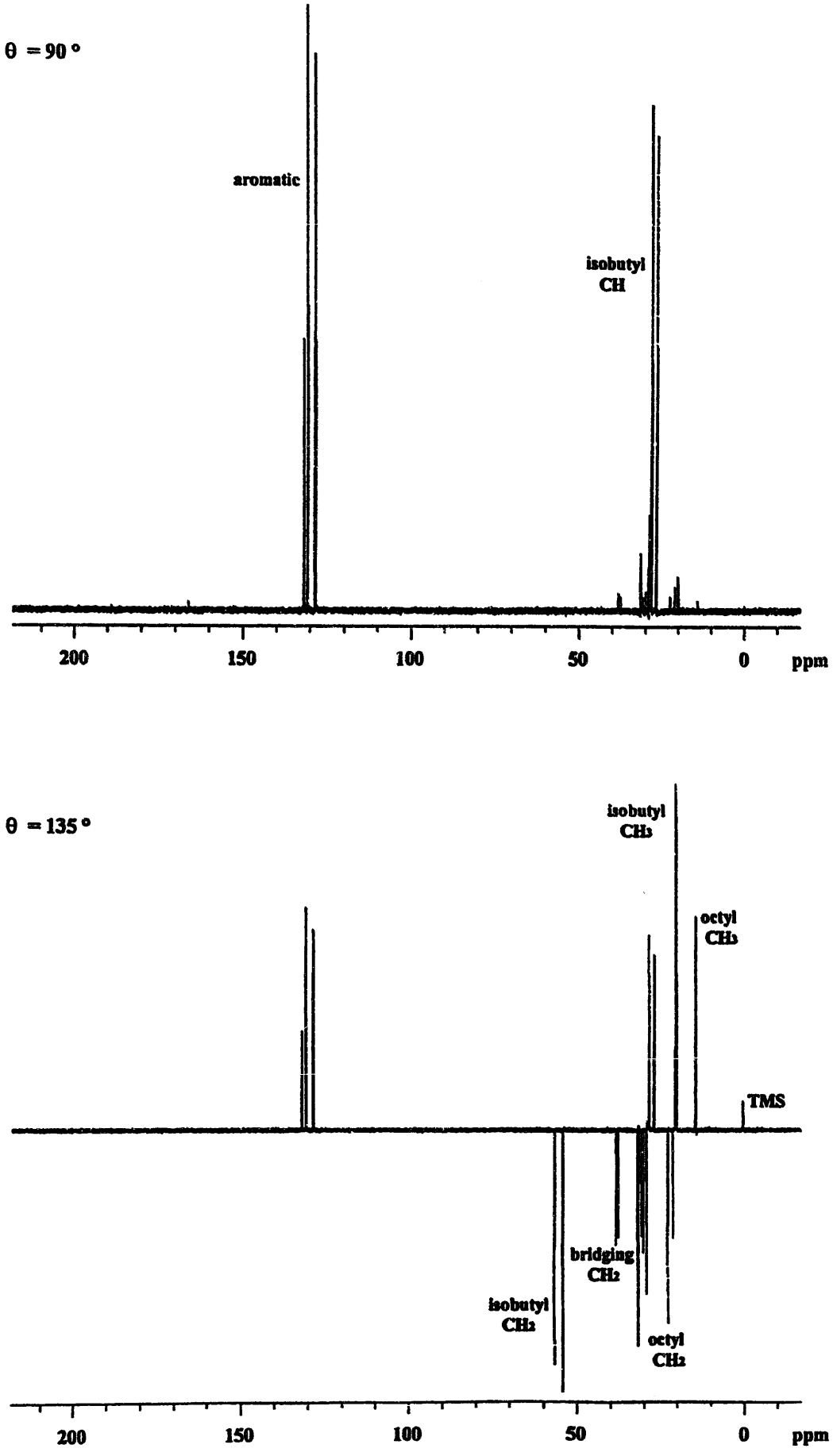

Fig. 3.6 (b) **^{13}C-NMR DEPT spectra of CMPO at room temperature.**

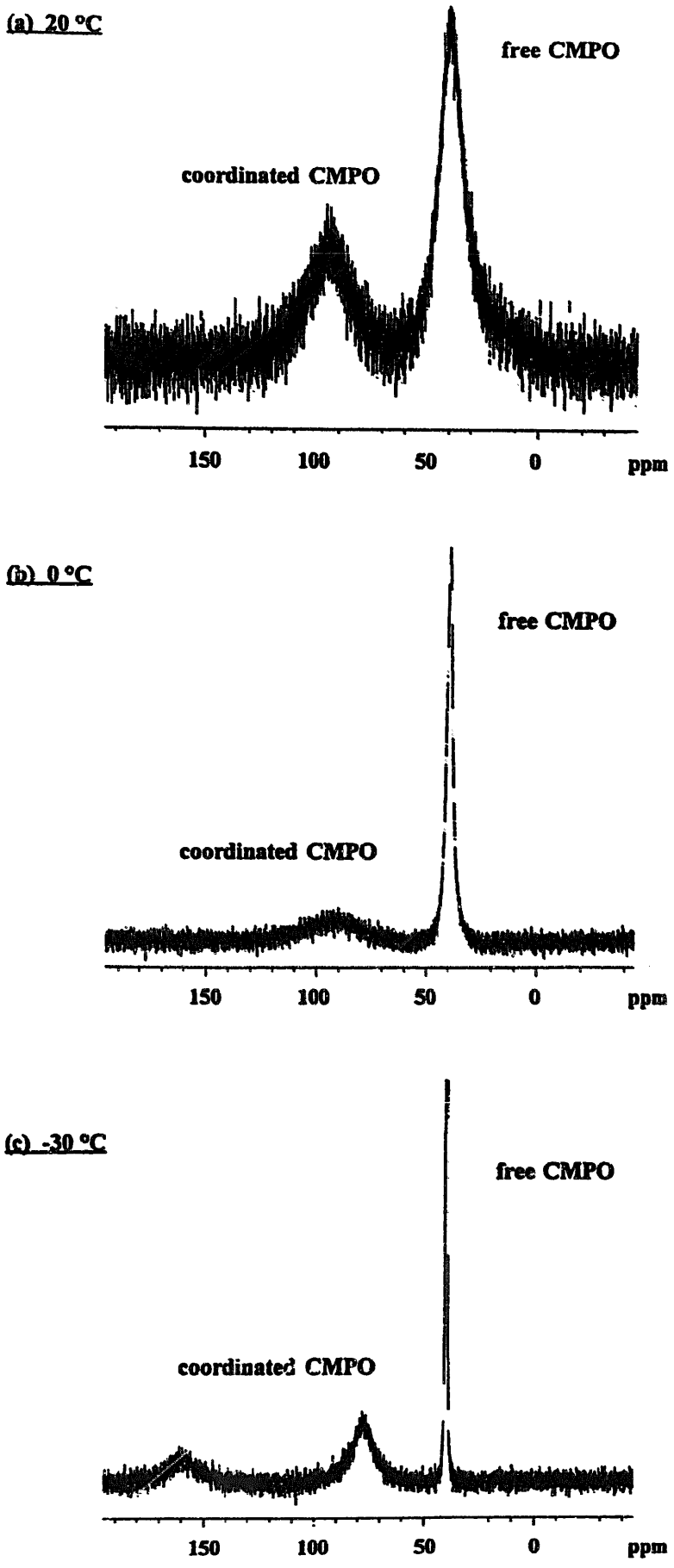

Fig. 3.7 Temperature dependence of ^{31}P-NMR spectra in Nd/CMPO system. Concentrations of Nd and CMPO are 0.087M and 0.62M, respectively.

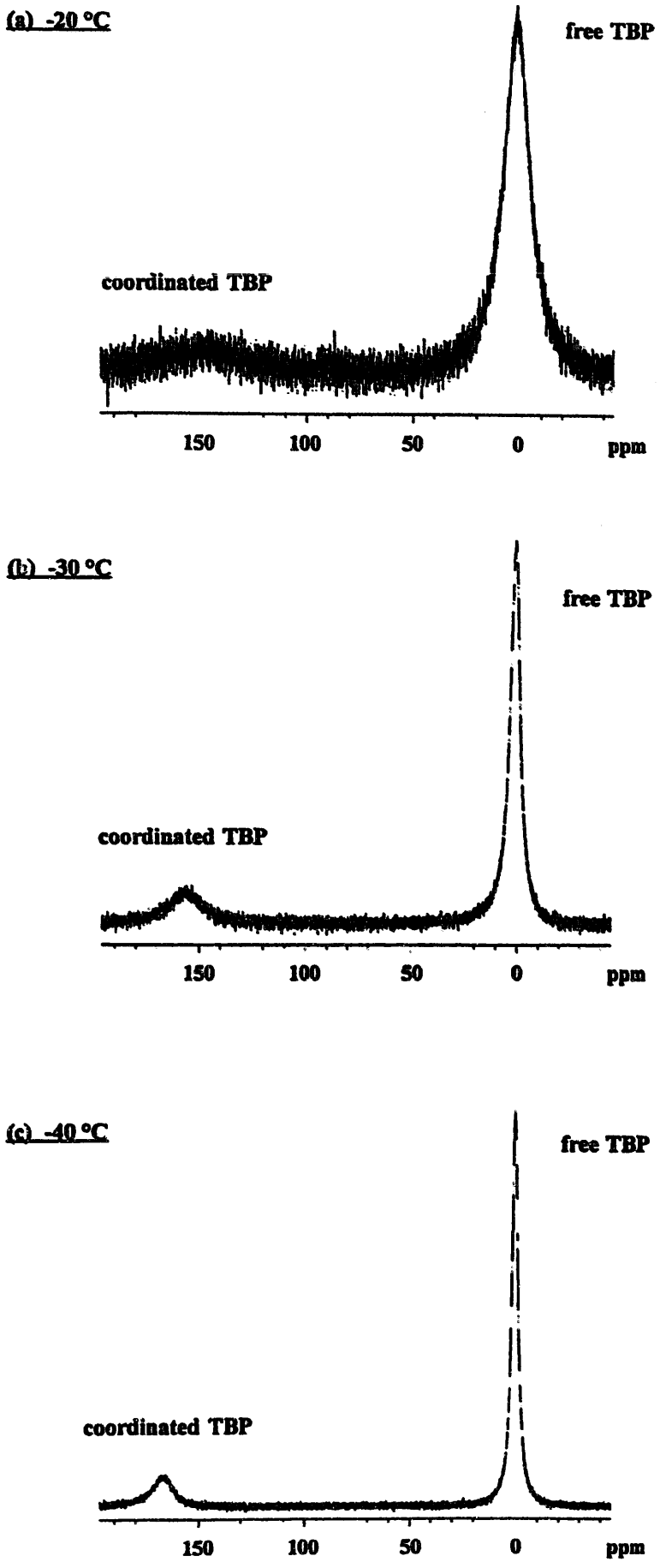

Fig. 3.8 Temperature dependence of ^{31}P-NMR spectra in Nd/TBP system. Concentrations of Nd and CMPO are 0.087M and 0.93M, respectively.

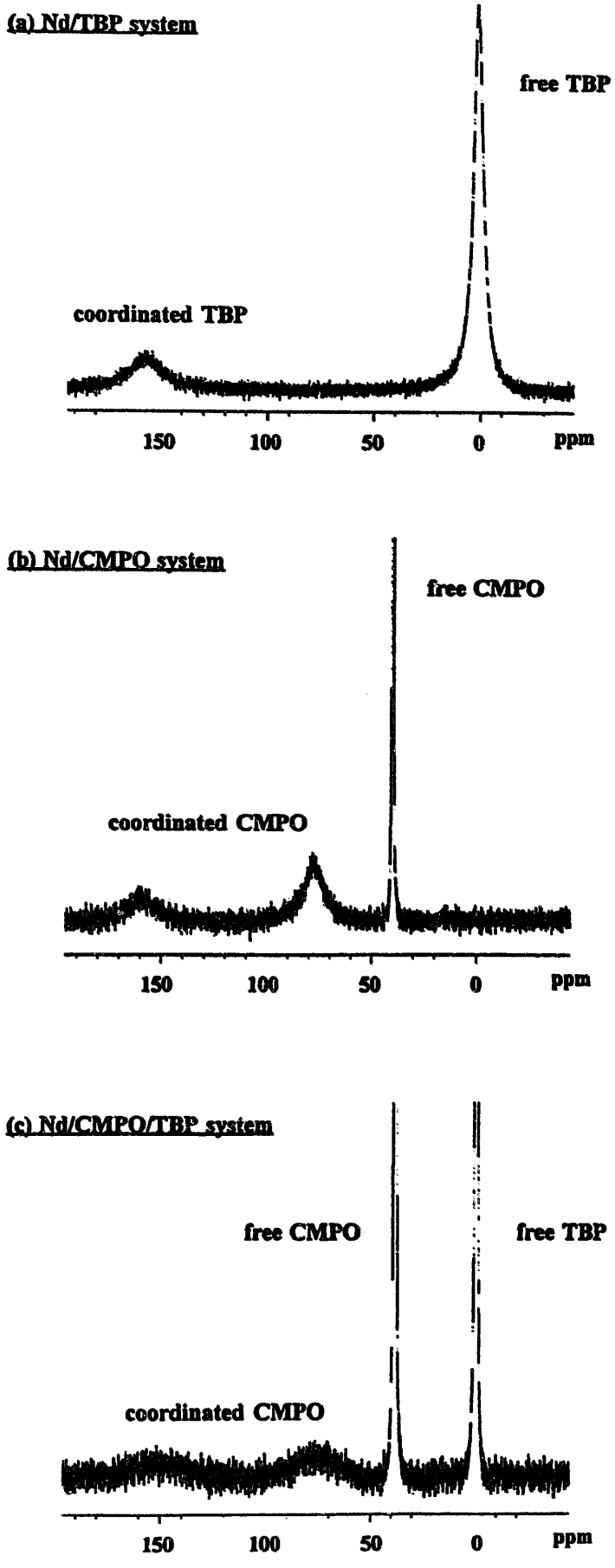

Fig. 3.9 **^{31}P-NMR spectra in Nd/TBP, Nd/CMPO and Nd/CMPO/TBP systems at -30 °C. Concentrations of Nd, TBP and CMPO are 0.087M, 0.94M and 0.62M, respectively.**

(a) Eu/TBP system

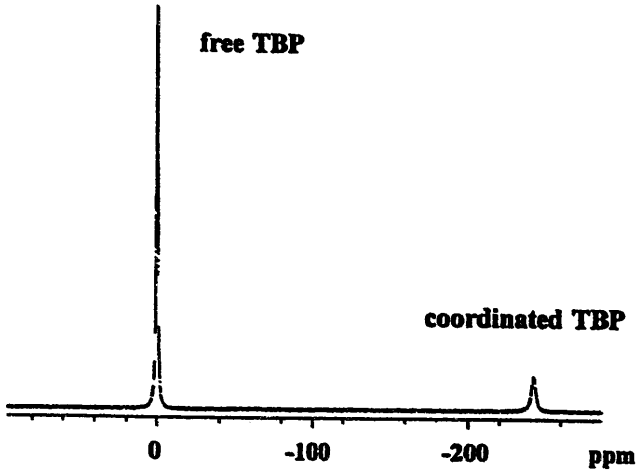

(b) Eu/CMPO system

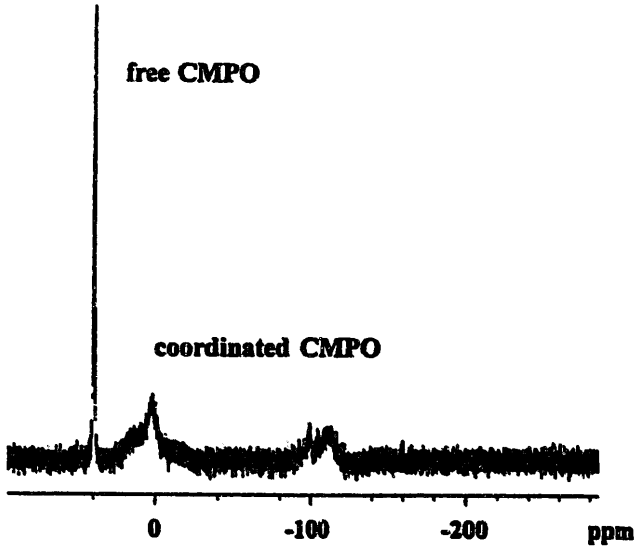

(c) Eu/CMPO/TBP system

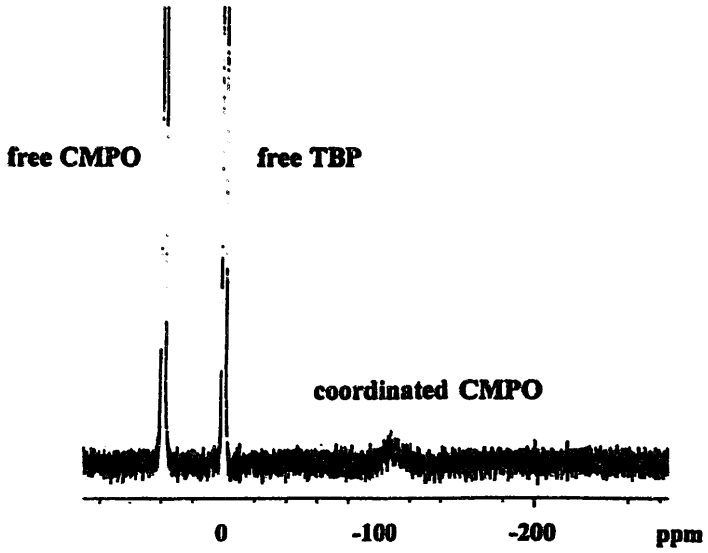

Fig. 3.10 **^{31}P-NMR spectra in Eu/TBP, Eu/CMPO and Eu/CMPO/TBP systems at -40 °C. Concentrations of Eu, TBP and CMPO are 0.086M, 0.94M and 0.62M, respectively.**

(a) Sm/CMPO system

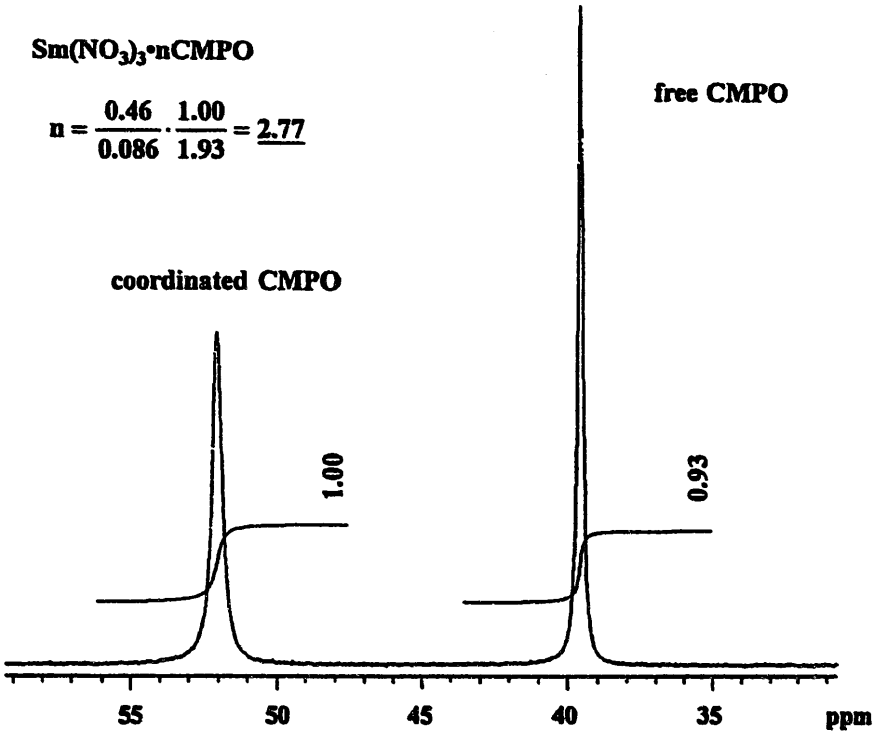

(b) Sm/CMPO/TBP system

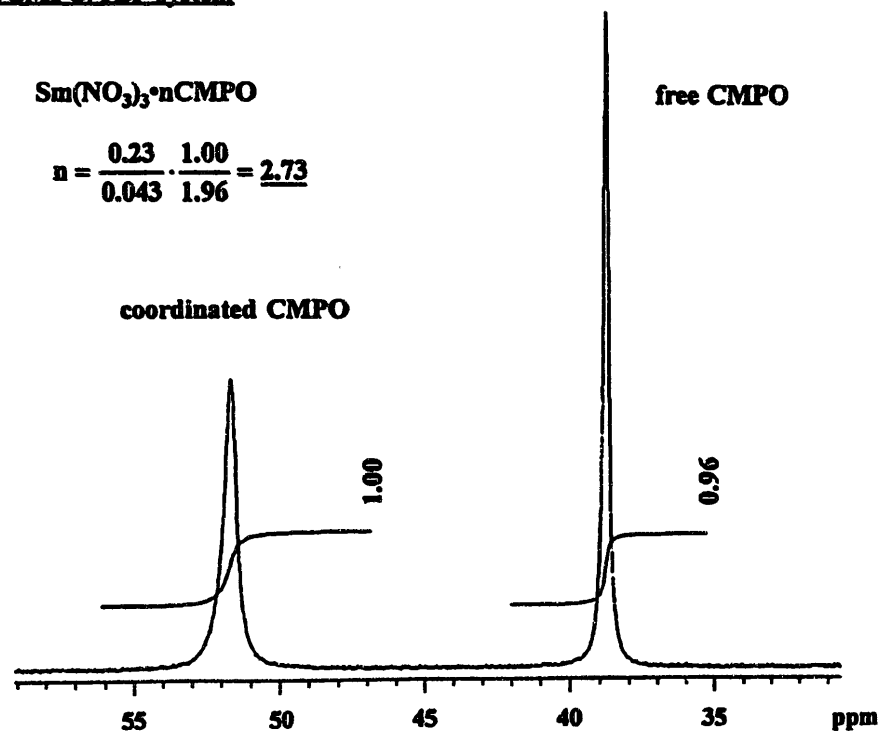

Fig. 3. 11 **^{31}P-NMR spectra of free and coordinated CMPO in Sm/CMPO and Sm/CMPO/TBP systems.**
(a) Concentrations of Sm and CMPO are 0.086M and 0.46M, respectively.
(b) Concentrations of Sm, CMPO and TBP are 0.043M, 0.23M and 0.94M, respectively.

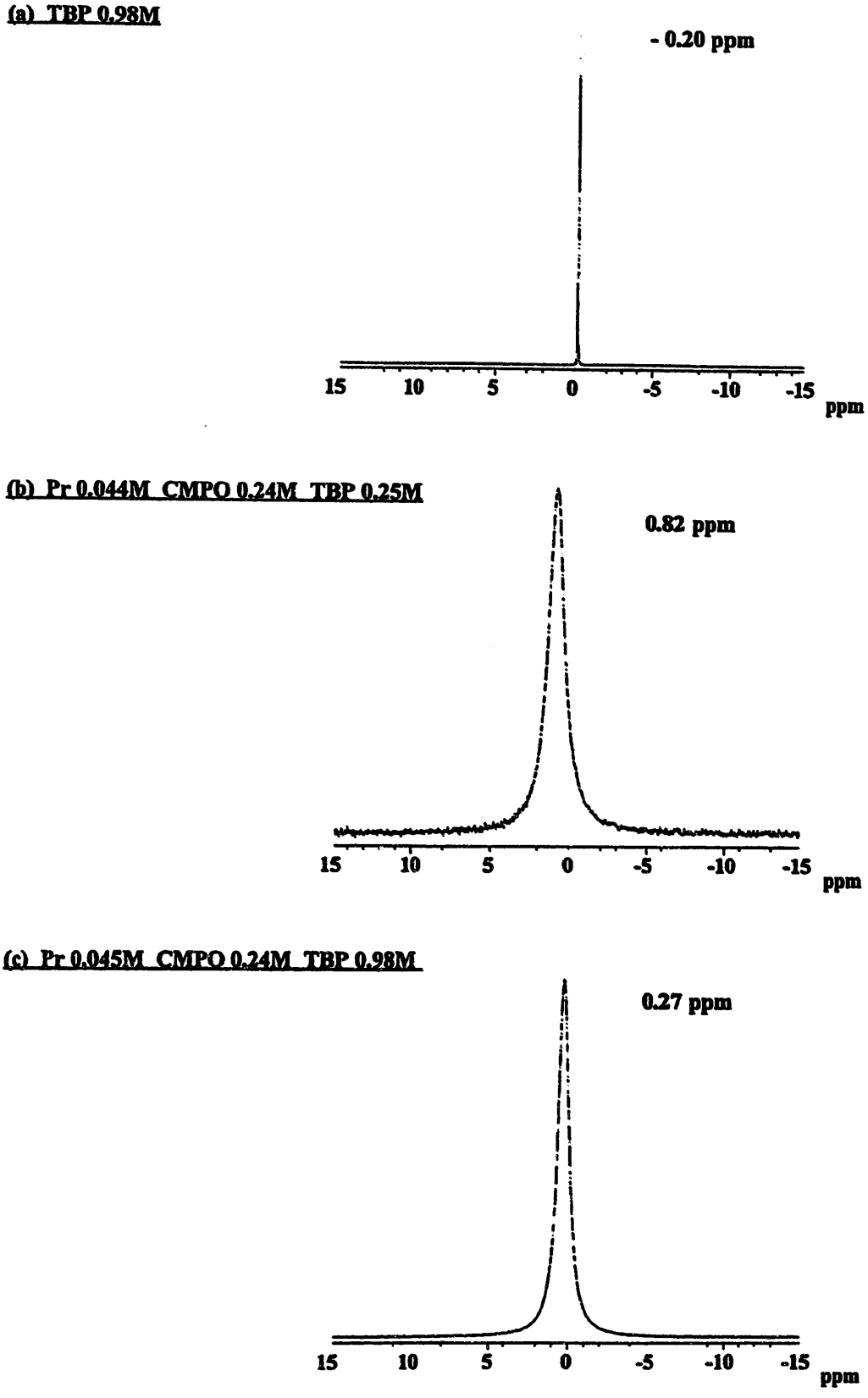

Fig.3.12 ^{31}P-NMR spectra of TBP in Pr/CMPO/TBP systems at 10 °C.

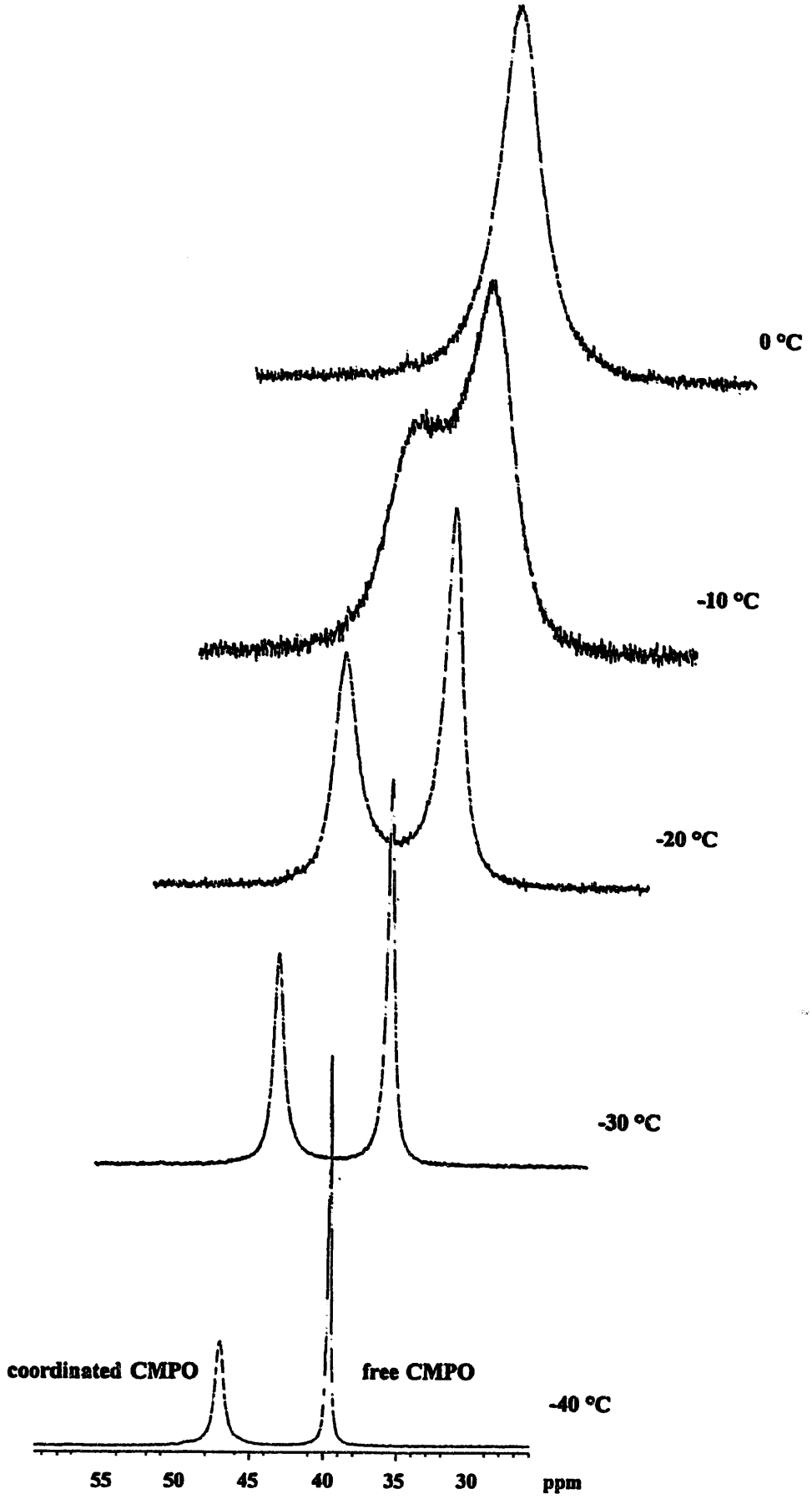

Fig. 3.13 Temperature dependence of ^{31}P-NMR spectra in La/CMPO system. Concentrations of La and CMPO are 0.086M and 0.62M, respectively.

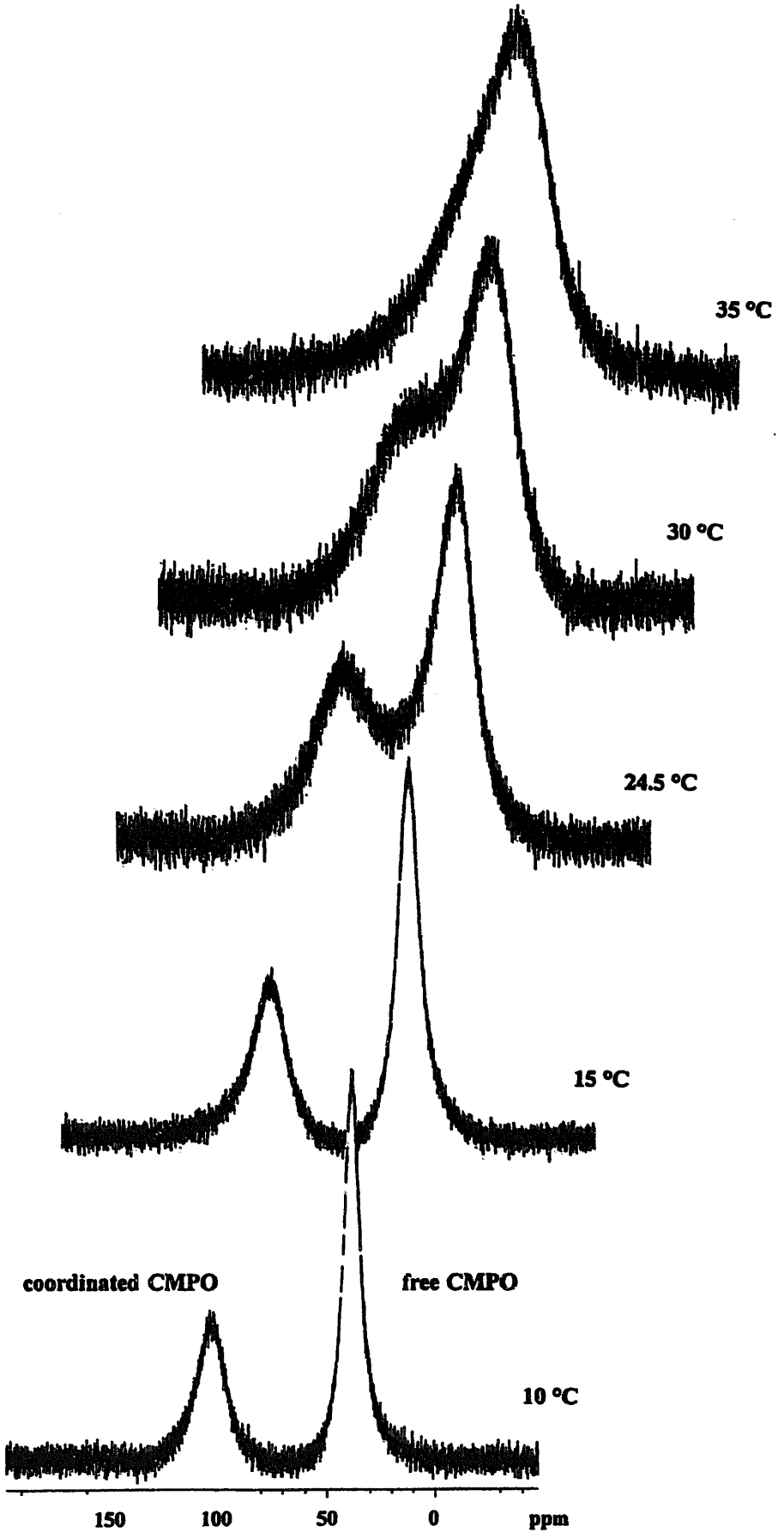

Fig. 3.14 Temperature dependence of ^{31}P-NMR spectra in Pr/CMPO system. Concentrations of Pr and CMPO are 0.088M and 0.62M, respectively.

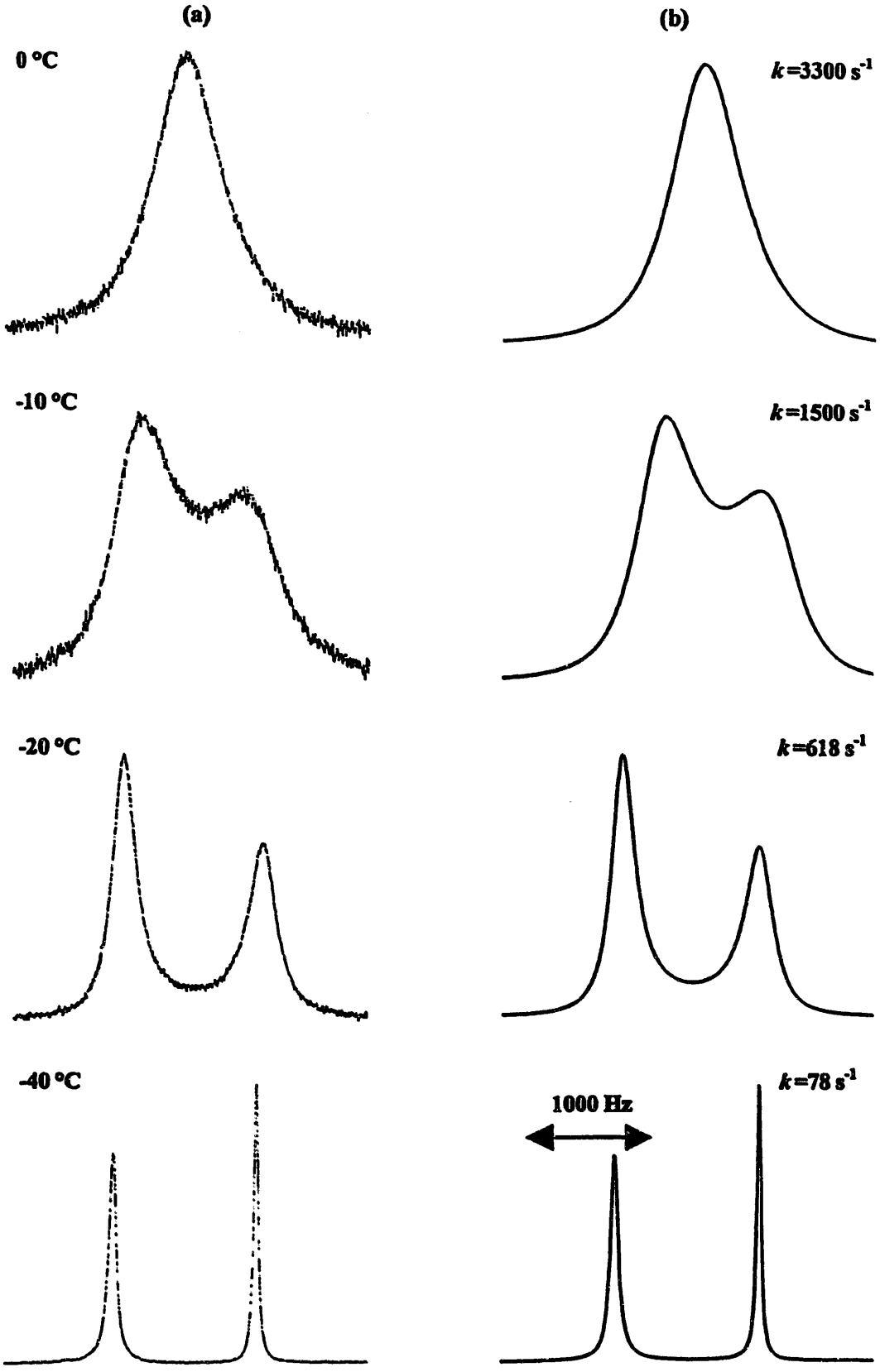

Fig. 3.15 **(a) Experimental 161.7MHz ^{31}P-NMR spectra in La/CMPO system. Concentrations of La and CMPO are 0.086M and 0.47M, respectively. (b) Simulated best-fit spectra and derived k values.**

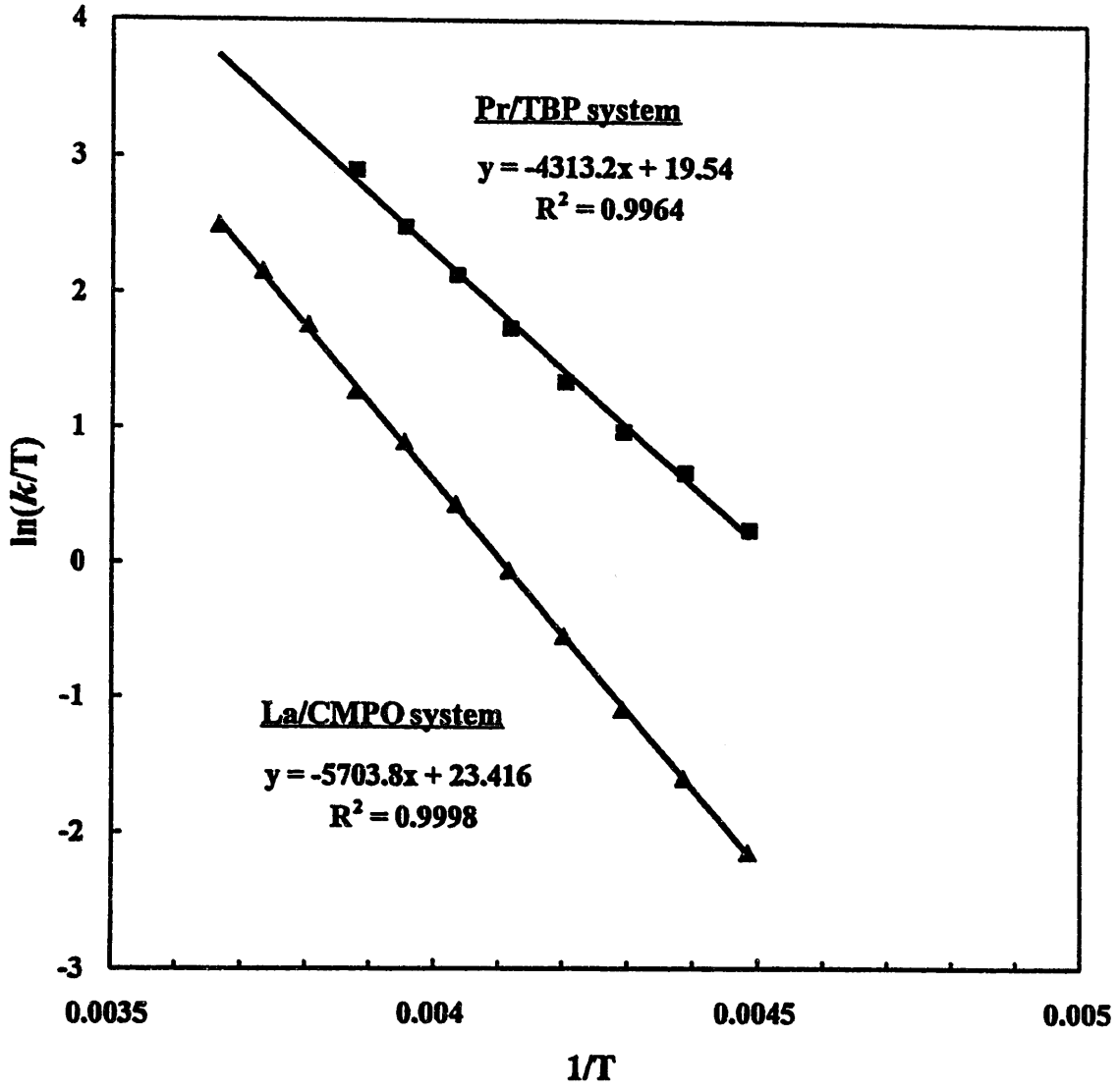

Fig. 3.16 Temperature dependence of ln(k/T) for ligand exchange reactions in Pr/TBP and La/CMPO systems.

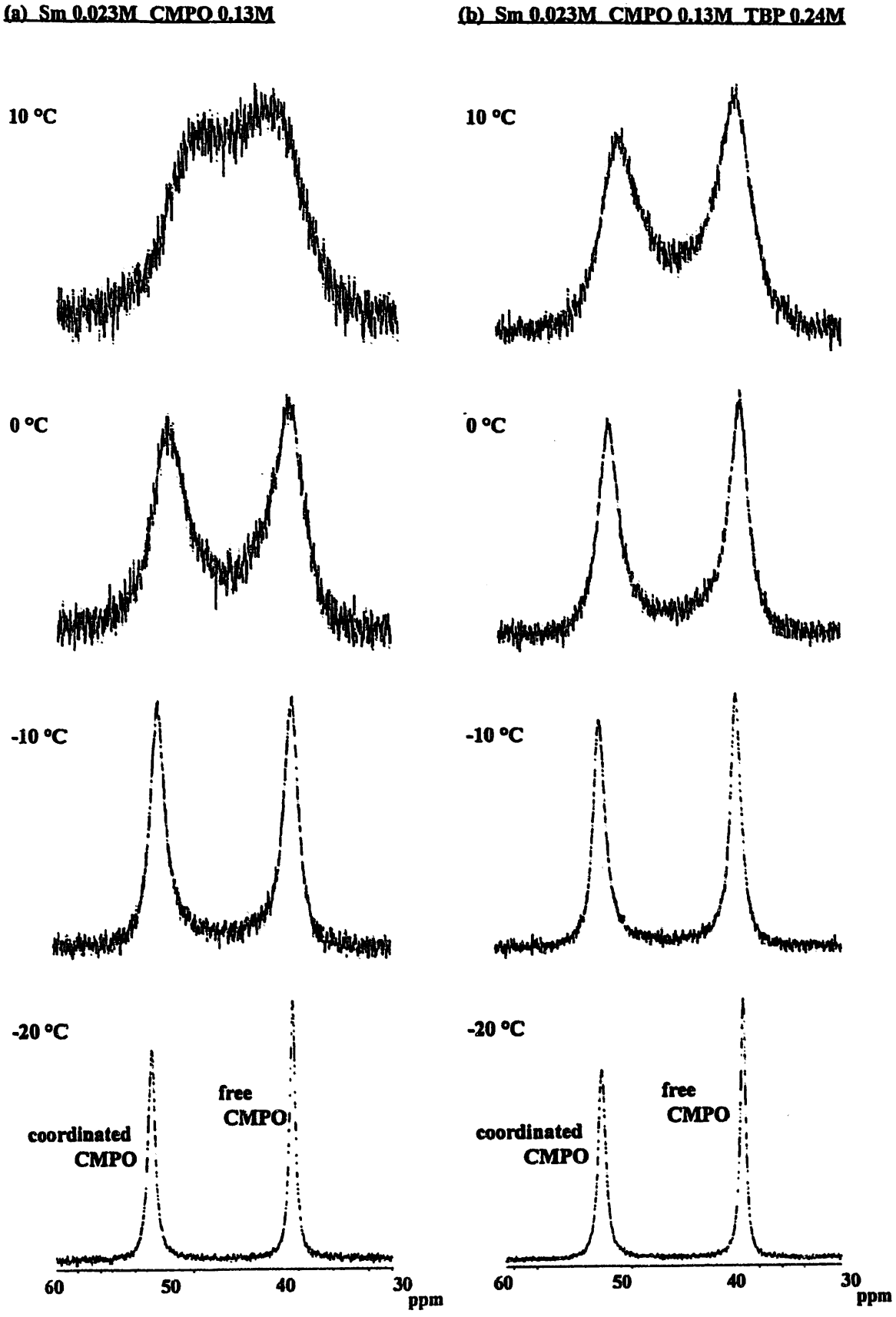

Fig. 3.17 Temperature dependence of ^{31}P-NMR spectra for free and coordinated CMPO in Sm/CMPO and Sm/CMPO/TBP systems.